Ultrafine Tin Nanocrystallites Encapsulated in Mesoporous Carbon Nanowires: Scalable Synthesis and Excellent Electrochemical Properties for Rechargeable Lithium Ion Batteries

Yongcai Qiu, Keyou Yan, Shihe Yang*

Supporting Information Available:

Experiment Section

Synthesis of Sn(IV) acetate nanowires. Commercial tin powder was allowed to react with an excess of acetic acid anhydride under agitation and at a temperature of 110°C. During the reaction, a flow of compressed air was passed through the reaction mixture. After cooling, the precipitate was filtrated and washed with ethanol several times, then dried in a vacuum at 60 ^{o}C for 10 h.

Synthesis of the UTP@CW and TP@CS precursors. 1 g of Sn(IV) acetate (or commercial SnO_2 powder with a mean particle diameter of 20 nm for preparation of TP@CS precursor) was dispersed in 20 mL DI water by ultrasonication to form a suspension. 2 g of glucose was dissolved in another 15 mL DI water, and the former suspension and another 25 mL of ethanol were added to the solution under gentle stir. The resulting suspension was transferred to a 100 mL teflon autoclave, which was then heated at 160 ^{o}C in an electric oven for 10 h. Afterward, the UTP@CW precursor (or TP@CS precursor) was harvested by centrifugation and washed with DI water, and finally dried at 100 ^{o}C in an oven.

Synthesis of Sn@carbon composites. The collected precursors were put in a tube furnace and calcined at 900^{o}C in Ar (93 vol%)/H_2 (7 vol%) for 6 h to obtain different Sn@C composite (UTP@CW and TP@CS). The heating rate was 2^{o}C min^{-1}.

Characterization. The as-prepared products were characterized by scanning electron microscopy (SEM), transmission electron microscopy (TEM) and powder X-ray diffraction (XRD) measurements. The morphologies were directly examined by SEM using a JEOL 6700F at an accelerating voltage of 5 kV. For TEM observations, the as-synthesized nanostructures were ultrasonically dispersed in ethanol and then dropped onto carbon-coated copper grids. TEM observations were carried out on JEOL 2010F and JEOL 2010 microscopes both operating at 200 kV. An energy-dispersive X-ray spectrometer (EDS) was attached to the JEOL 2010F. The XRD analyses were performed on a Philips PW-1830 X-ray diffractometer with Cu Ka radiation (λ = 1.5406 Å) at a scanning speed of 0.025°/sec over the 2θ range of 10–70°. Adsorption isotherms at 77 K were measured using an ASAP 2020 apparatus.

LIB electrode fabrication and performance measurements. The electrodes were fabricated by using the Sn/C nanocomposites as the active materials, Super-P and polyvinylidene fluoride (PVDF) binder in a weight ratio of 80:10:10. The slurry was coated on a copper foil and dried overnight in a vacuum at 100°C. For cell test, the electrode was cut into a square shape with an area of 1 cm^2. The electrochemical performances of these electrodes were evaluated in a 2016 coin-type cell, in which the lithium electrode was used as the counter electrode as well as the reference electrode.

The electrolyte was 1 M $LiPF_6$ in ethylene carbonate (EC) and diethyl carbonate (DEC) (1:1 by volume). All the cells were assembled in an argon-filled glove box. All electrochemical measurements were conducted on Autolab (PGSTAT-30, Eco Echemie B.V. Company).

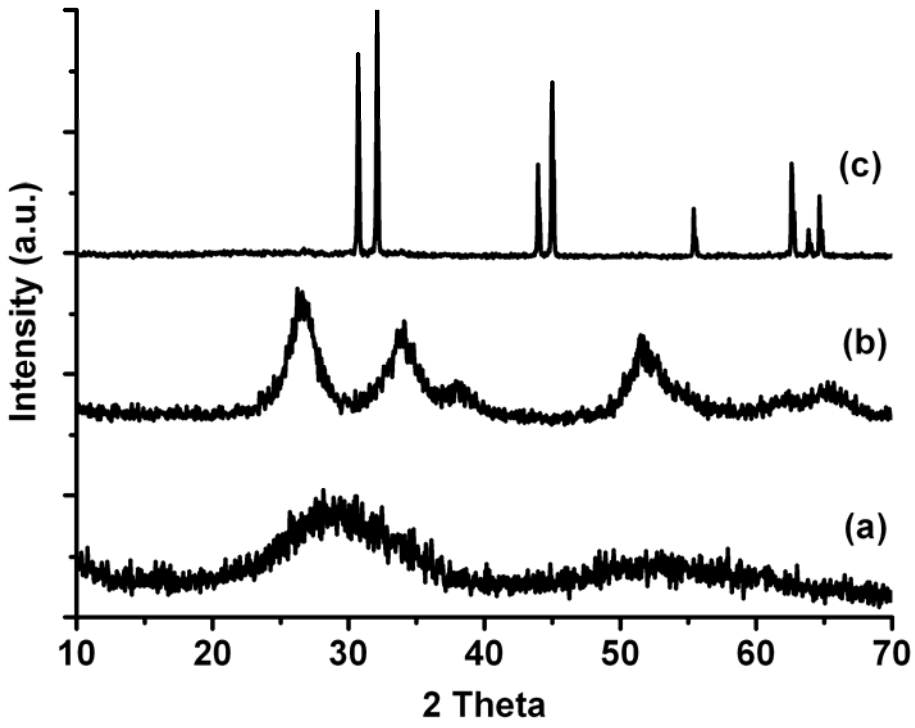

Figure S1. XRD patterns of the as-prepared Sn(IV) acetate nanowires (a), SnO_2@CW - the sample obtained after hydrothermal treatment of the Sn(IV) acetate nanowires in the presence of glucose (b), and the UTP@CW (c).

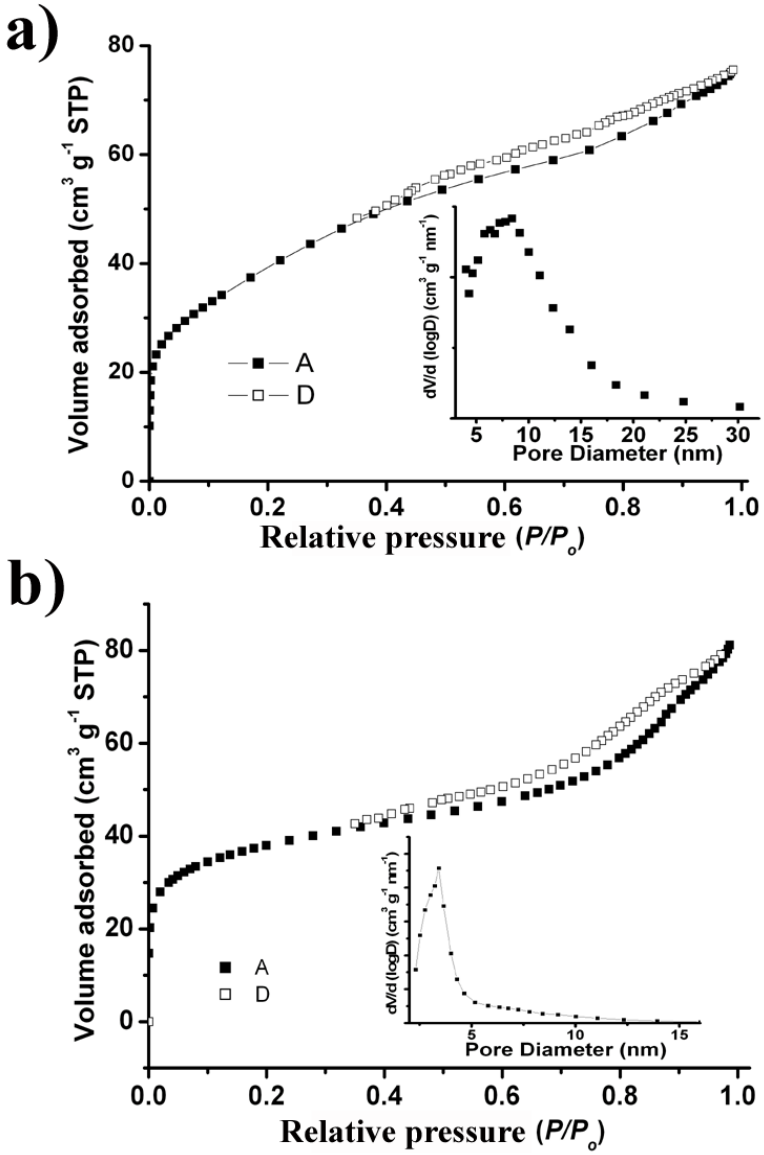

Figure S2. Nitrogen adsorption–desorption isotherms of the samples before reduction (a) and after reduction (b) of the precursor of UTP@CW. The inset shows their pore size distribution calculated by BJH method.

The pore structure and surface area of the samples before reduction (a) and after reduction (b) of the precursor of UTP@CW was investigated by nitrogen adsorption-desorption method (Figure S2a nad S2b). A type IV isotherm with a capillary condensation step at high relative pressures is observed for both samples and a hysteresis loop near relative pressure of ~0.60 in the desorption branch indicates the presence of mesopores. As observed from the inset of Figure S2a nad S2b, the pore size distribution for the sample before reduction ranges from 3.6 to 30 nm. After reduction, however, it changes from 2.5 to 10 nm most likely due to the shrinkage of the nanowires. The measured BET areas of the samples before reduction and after reduction are ~131 and ~154 m^2 g^{-1}, respectively.

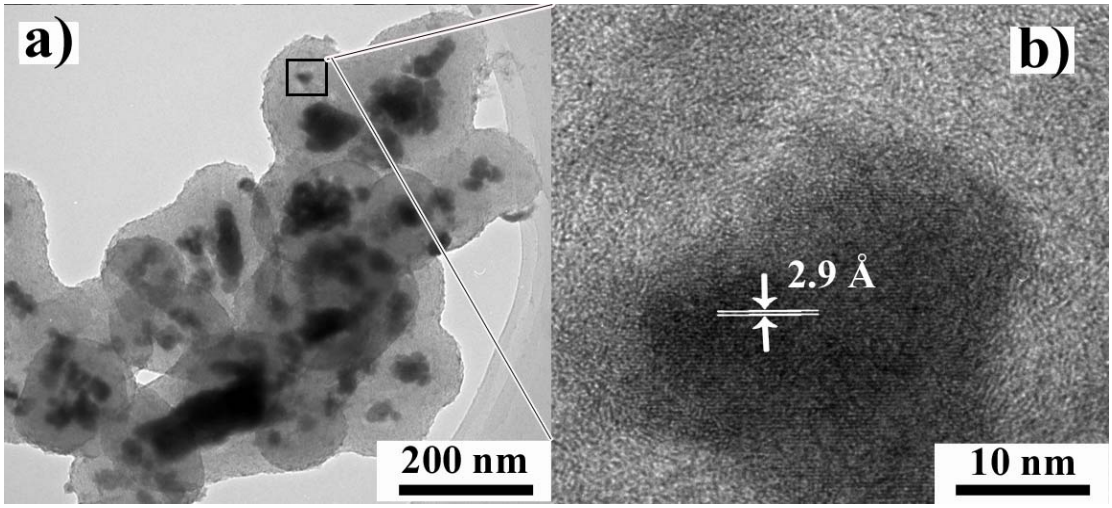

Figure S3. (a) TEM image and (b) a close-up image of metallic tin encapsulated in carbon spheres (TP@CS) after heat treatment of a SnO_2 encapsulated carbon precursor in an Ar/H_2 flow (see Experimental Section for details).

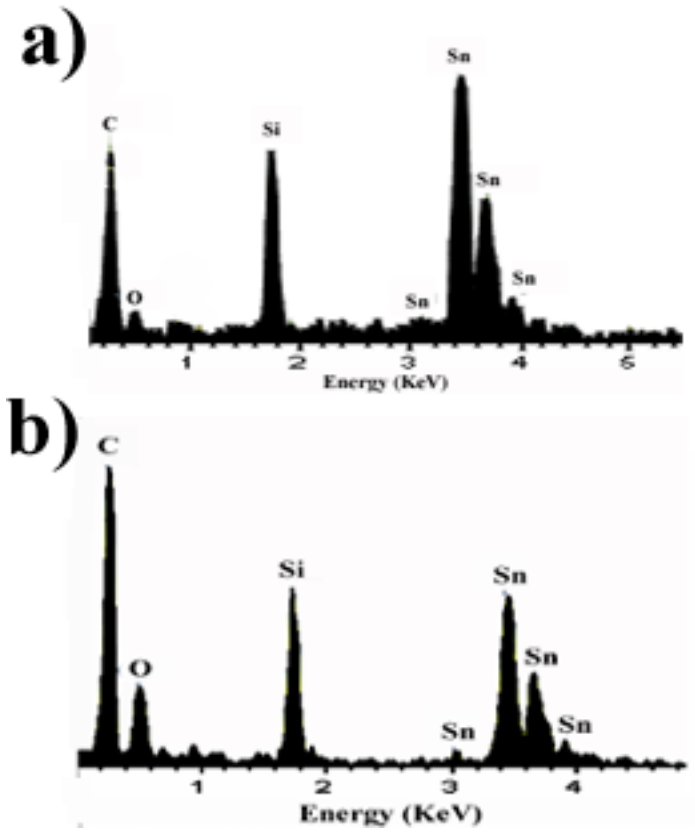

Figure S4. SEM EDX spectra of the UTP@CW (a) and TP@CS (b). Detailed compositions from this analysis are shown in Table S1.

Table S1. Detailed chemical compositions from SEM EDX analyses of the UTP@CW and TP@CS.

UTP@CW			**TP@CS**		
Element (Shell)	**Weight%**	**Uncertainty (Weight%)**	**Element**	**Weight%**	**Uncertainty (Weight%)**
C (K)	**21**	**0.5**	**C K**	**34**	**0.6**
O (K)	**2**	**0.6**	**O K**	**3**	**0.8**
Sn (L)	**77**	**0.8**	**Sn L**	**63**	**0.6**

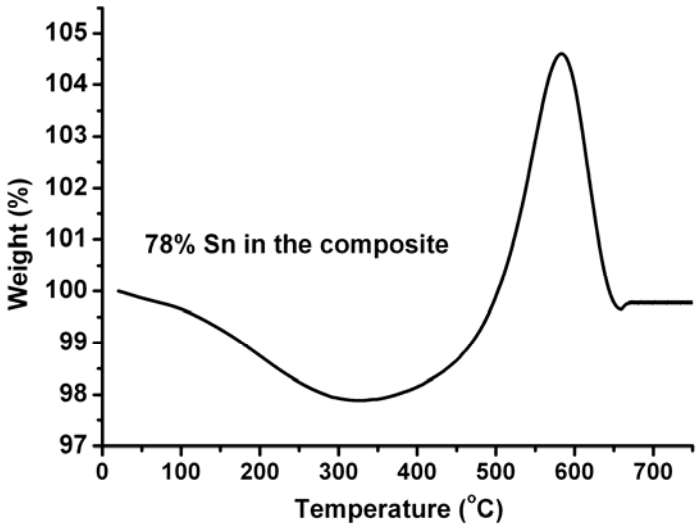

Figure S5. Thermal analysis (TGA) of the UTP@CW further confirms the presence of metallic Sn. The Sn content estimated from the thermal analysis is ~78% wt (The final residue after combustion above 650°C is SnO_2, which is about 99.8 wt%, and the Sn content is equal to 99.8% times M_{sn}/M_{Sno2}). The thermal analysis was taken in air at a heating rate of 5°C min^{-1}. The weight loss from room temperature to 350°C is due to the removal of the adsorbed water and the combustion of amorphous carbon. The weight gain is due to oxidation of Sn to SnO_2. The subsequent weight loss from 600 °C to 650 °C is due to complete combustion of amorphous carbon.

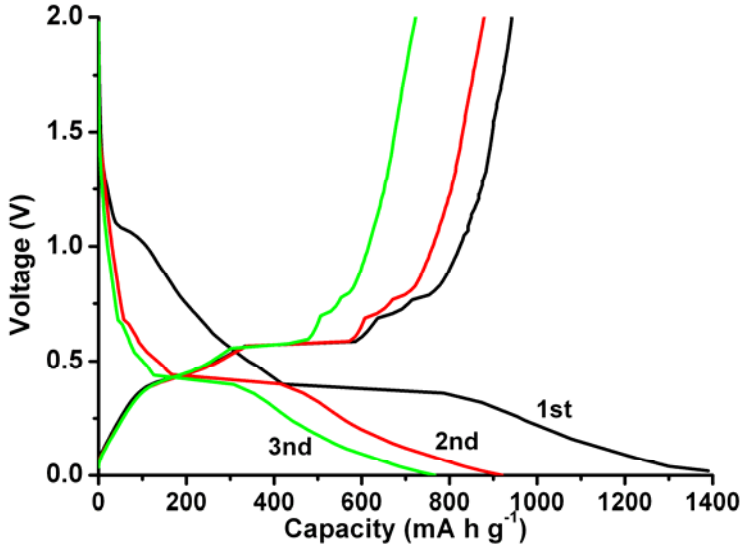

Figure S6. Charge and discharge curves of the UTP@CW at 100 mA g^{-1} in the voltage window of 5 mV–2.0 V (*vs.* Li^+/Li).